Interpretation of Specular X-ray Reflectivity Profiles of Langmuir–Blodgett Films

Shin Takahashi [1,2], Satoko Yamashita [2] Masahiro Taniguchi [3], and Akihiko Yamagishi [4]

[1] National Institute for Materials Science, Tsukuba 305-0047, Japan
Fax: +81-29-859-2801, e-mail: shin@yuhgiri.nims.go.jp
[2] Graduate School of Science, Hokkaido University, Sapporo 060-0810, Japan
[3] Department of Materials Science and Engineering, Kanazawa Institute of Technology, Ishikawa 921-8501, Japan
[4] Graduate School of Science, The University of Tokyo, Tokyo 113-0033, Japan

Specular X-ray reflectometry has been applied to evaluate molecular orientation in the Langmuir–Blodgett (LB) film which consists of amphiphilic ruthenium complex derivatives, $[Ru(bpy)_2(dC18bpy)]^{2+}$ or $[Ru(phen)_2(dC18bpy)]^{2+}$ (bpy = 2,2'-bipyridine, dC18bpy = 4,4'-dioctadecyl-2,2'-bipyridine, phen = 2,2'-phenantrolline). For the analyses of reflectivity profiles, Parratt formalism was used by assuming two structural models that the orientation of molecules is completely random in the vertical direction to a surface(model I) or highly ordered molecules (model II). As a result, model I reproduced the observed profiles with the parameters consistent with the actual physical properties of composite layers. Thus we conclude that specular X-ray reflectometry gave information on the electron density contrast even in a monolayer. Although there are some problems still to be solved, the present approach is expected to provide a useful tool for analyzing a molecular orientation on a surface.

Key words: specular X-ray reflectivity, molecular orientation, Langmuir – Blodgett film, electron density profile

1. INTRODUCTION

An interfacial surface plays an important role in wide disciplines not only in academic interest but also for industrial use, since most of chemical reactions occur at surfaces. Recently, there has been growing importance of surface phenomena from the viewpoint of nano-scale technology. In order to study the mechanisms of various surface phenomena on atomic or molecular scales, it is required to evaluate surface structure as well as buried interface structure by constructing a highly ordered surface modified with functional molecules. For evaluating molecular orientation in a vertical direction to the surface, a number of spectroscopic techniques such as infrared reflection absorption spectroscopy [1 – 5] and infrared–visible light sum or difference frequency generation spectroscopy [6 – 8] are well known as a powerful tool. These techniques are sensitive to orientation angle of transition moment of intra-molecular vibration, for instance CH_2 stretching vibration, by use of *p*- or *s*-polarized infrared or visible light. Nowadays these have been developed as an essential technique to evaluate molecular orientation on a certain kind of surface or interface and widely applied to various scientific fields such as catalytic chemistry, biological chemistry and chemical physics. Especially, catalytic chemistry has been advanced by in–situ spectroscopic techniques [4 – 5, 7 – 8]. However, there are some problems that are difficult to be solved. For example, only few vibration modes in a molecule are applicable due to limitation of wave-number region of light, or it is often the case that spectra were very complicated due to the overlapping of absorption peaks or by optical properties of samples and substrates. In addition, those techniques do not reflect layer structure

around a surface. In order to complement such problems, we attempted to apply grazing incidence specular X-ray reflectometry. Sometimes it is considered as an evaluation technique not for molecular orientation but for layer structure or interface structure. Much works of surface and interface structure have been carried out by such X-ray technique [9 – 17]. For instance, we also reported layer structure in organic–inorganic hybrid films by means of specular X-ray reflectometry [16]. This is due to its high sensitivity to the change of electron density at an interface between layers. L. G. Parratt proposed a method to interpret specular X-ray reflectivity profile, treating a reflection as a multiple of Fresnel reflections from each boundary [9]. Specular X-ray reflectivity profiles will also reflect gradual electron density profile around a surface. For instance, a metal oxide layer naturally produced on metal is expected to have gradual changing of layer density. In this case, usually one layer is assumed as a multilayer constructed by some layers with different densities, allowing it to apply Parratt's optical theory. Here, we should note that a monolayer film consisting of highly ordered asymmetric molecules has electron density polarized to the direction of surface normal, i.e., it is likely to consider to have gradual change of electron density similar to the case of oxide layers.

It looks that Parratt's theory easily can be applied to various surfaces automatically and systematically. In the present report, we aimed to discuss molecular orientation, taking an electron density profile into account, by analysis of specular X-ray reflectometry on the basis of Parratt's theory.

For the present purpose, a monolayer Langmuir–Blodgett (LB) films were used which are

likely to consider as a good example, since it is expected the presence of polarization in the film, being caused by ordering of an asymmetric molecule composed with hydrophobic and hydrophilic groups. In such a case, specular X-ray reflectivity profile may reflect electron density profile even in the monolayer film.

2. EXPERIMENTAL

Monolayer LB films of amphiphilic ruthenium complex derivatives, [Ru(bpy)$_2$(dC18bpy)]$^{2+}$(ClO$_4$)$_2$ and [Ru(phen)$_2$(dC18bpy)]$^{2+}$(ClO$_4$)$_2$ (bpy = 2,2'-bipyridine, dC18bpy = 4,4'-dioctadecyl-2,2'-bipyridine, phen = 2,2'-phenantrolline), were used in the present work. Molecular models are shown in Figs. 1 (a) and (b), respectively. Two alkyl chains (denoted as tail groups) are introduced on one of the ligands in order to flow on water surface. The ruthenium complex is hydrophilic group (denoted as head group) with diameter of around 1.0 nm. Each sample was dissolved in chloroform solution as a spreading solvent. At 90min after spreading a sample solution onto 0.1 M NaClO$_4$ aqueous solution, a trough surface was compressed at a rate of 10cm^{2}min^{-1} up to a surface pressure of 15mN m^{-1}. The floating monolayer film was transferred onto a hydrophilic Si substrate by the vertical dipping method at the surface pressure of 15mN m^{-1}. The hydrophilic Si substrates (30mm×18mm) were obtained by being immersed in a mixed solution of 30% hydrogen peroxide and 25% ammonia water (1:1 v/v) at 80°C for 2 hours. Si substrates were taken from the same wafer (gifts from Shin-Etsu Chemical Co., Japan). All procedures for fabrication of films were done at 20°C. A film transfer ratio was up to 90%. Specular X-ray reflectivity (SXR) measurements were carried out by RINT 2100 diffractometer (Rigaku, Co., Japan) using a conventional X-ray source equipped with a graded *d*-spacing parabolic multilayered mirror. Specular X-ray reflectivity profiles were analyzed by fitting program RGXR (Rigaku, Co., Japan) that is based on optical theory developed by L. G. Parratt [9] with a roughness model proposed by P. Croce and L. Nevot [10].

3. RESULTS & DISCUSSION

Figs. 2 show SXR profiles of (a) Si substrate, (b) monolayer [Ru(phen)$_2$(dC18bpy)]$^{2+}$(ClO$_4$)$_2$ and (c) monolayer [Ru(bpy)$_2$(dC18bpy)]$^{2+}$(ClO$_4$)$_2$ LB films, respectively. As a first step, SiO$_2$ layer naturally produced on a Si surface was analyzed. Taking a density gradient of SiO$_2$ into account, the layer was divided into two layers. The obtained parameter values of SiO$_2$ layers are arranged in Table I. In both of the Ru complex LB films, broad peaks were observed in their SXR profiles at glancing incidence angle α = 2.5 ~ 4.0°. We assumed two models (denoted as I and II) as a structure model of Ru complex film as shown in Fig. 3. As is expected, the variation of electron density profile in the vertical direction to a surface was in accordance with molecular orientation. In all structure models, the SiO$_2$ layer was placed onto a pure Si surface. For simplicity in analyzing the SXR curves for Ru complex LB films, the values of SiO$_2$ layers as shown in Table I were used as fixed or initial parameters. This is because the Si substrates used in this study were prepared by being cut from the same wafer.
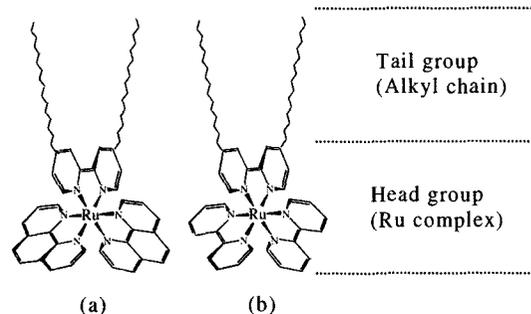
Figs. 1 (a) and (b). Molecular models of Ru complex derivatives, (a) [Ru(bpy)$_2$(dC18bpy)]$^{2+}$ and (b) [Ru(phen)$_2$(dC18bpy)]$^{2+}$, respectively.
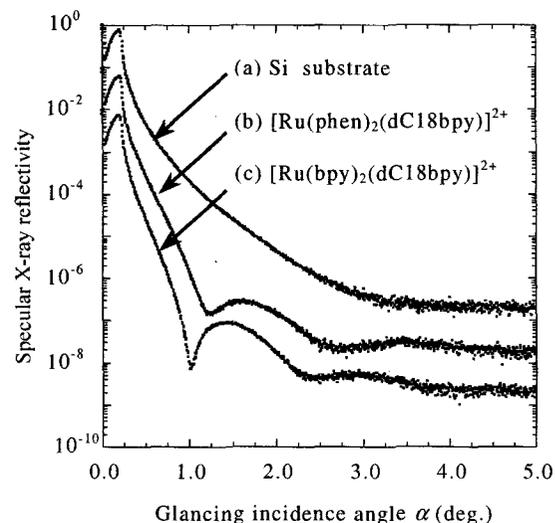
Figs. 2 (a), (b) and (c). SXR profiles of (a) Si substrate, (b) [Ru(bpy)$_2$(dC18bpy)]$^{2+}$(ClO$_4$)$_2$ LB film and (c) [Ru(phen)$_2$(dC18bpy)]$^{2+}$(ClO$_4$)$_2$ LB film, respectively.

Table I. Fitting results of Si substrate. Two SiO$_2$ layers were put on Si substrate.

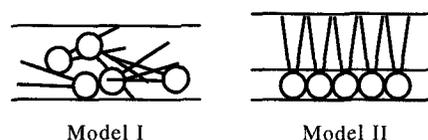| Layer	Density (g/cm^3)	Thickness (nm)	Roughness (nm)
SiO$_2$	1.77	0.47	0.30
SiO$_2$	2.17	0.53	0.15
Si	2.33	---	0.00

Fig. 3. Structure models of a monolayer film on Si substrate, depending on molecular orientation. Models I and II show perfectly disordered molecules and highly ordered molecules in a monolayer film, respectively.

Figs. 4 (a) and (b) are fitting curves when a model I are applied as a structure model for both SXR profiles of Ru complex LB films by use of constant parameters for SiO$_2$ layers, respectively. The obtained parameters are arranged in Tables II (a) and (b), respectively. Interference oscillation pattern appearing at the glancing
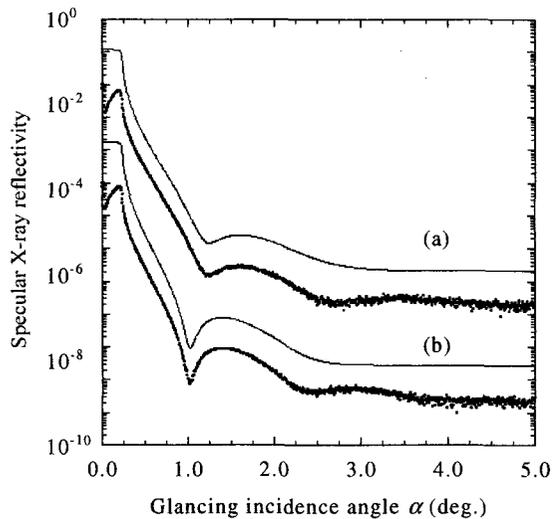
Figs. 4 (a) and (b). Fitting curves applying a model I to SXR profiles of (a) [Ru(phen)$_2$(dC18bpy)]$^{2+}$(ClO$_4$)$_2$ LB film and (b) [Ru(bpy)$_2$(dC18bpy)]$^{2+}$(ClO$_4$)$_2$ LB film, respectively. In both fitting curves were given off set in reflectivity for clear illustration.

Figs. 5 (a) and (b). Fitting curves applying a model II to SXR profiles of (a) [Ru(phen)$_2$(dC18bpy)]$^{2+}$(ClO$_4$)$_2$ LB film and (b) [Ru(bpy)$_2$(dC18bpy)]$^{2+}$(ClO$_4$)$_2$ LB film, respectively. In both fitting curves were given off set in reflectivity for clear illustration.

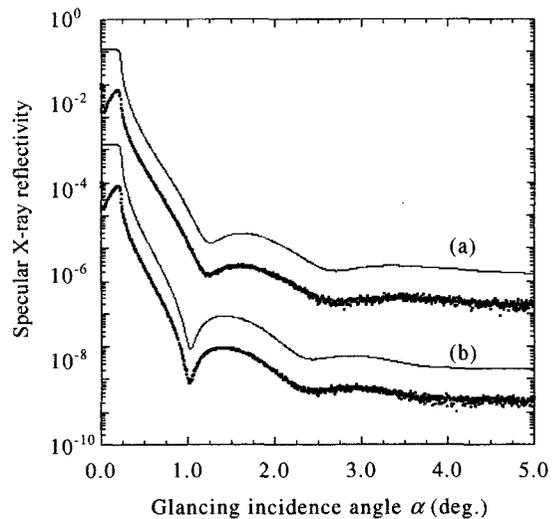Table II (a). Fitting results with model I for [Ru(phen)$_2$(dC18bpy)]$^{2+}$(ClO$_4$)$_2$ LB film. Parameters of SiO$_2$ layers were fixed at constant values shown in Table 1. The values put in square bracket are results obtained in the case that SiO$_2$ layers were also added as fitting parameters.

Layer	Density (g/cm^3)	Thickness (nm)	Roughness (nm)
Complex	1.59 (1.23)	1.29 (1.21)	0.65 (0.47)
SiO$_2$	1.77 (1.88)	0.47 (0.41)	0.30(0.30)
SiO$_2$	2.17 (1.71)	0.53 (0.60)	0.15 (0.34)
Si	2.33	---	0.00

Table III (a). Fitting results with model II for [Ru(phen)$_2$(dC18bpy)]$^{2+}$(ClO$_4$)$_2$ LB film. Parameters of SiO$_2$ layers were fixed at constant values shown in Table 1. The values put in square bracket are results obtained in the case that SiO$_2$ layers were also added as fitting parameters.

Layer	Density (g/cm^3)	Thickness (nm)	Roughness (nm)
Tail group	0.64 (0.63)	1.11 (1.11)	0.21 (0.22)
Head group	1.12 (1.13)	0.74 (0.74)	0.00 (0.18)
SiO$_2$	1.77 (1.78)	0.47 (0.53)	0.30 (0.31)
SiO$_2$	2.17 (2.22)	0.53 (0.63)	0.15 (0.10)
Si	2.33	---	0.00

Table II (b). Fitting results with model I for [Ru(bpy)$_2$(dC18bpy)]$^{2+}$(ClO$_4$)$_2$ LB film. Parameters of SiO$_2$ layers were fixed at constant values shown in Table I. The values put in square bracket are results obtained in the case that SiO$_2$ layers were also added as fitting parameters.

Layer	Density (g/cm^3)	Thickness (nm)	Roughness (nm)
Complex	1.23 (0.98)	1.86 (1.78)	0.68 (0.31)
SiO$_2$	1.77 (1.86)	0.47 (0.96)	0.30 (0.36)
SiO$_2$	2.17 (2.47)	0.53 (1.59)	0.15 (0.00)
Si	2.33	---	0.00

Table III (b). Fitting results with model II for [Ru(bpy)$_2$(dC18bpy)]$^{2+}$(ClO$_4$)$_2$ LB film. Parameters of SiO$_2$ layers were fixed at constant values shown in Table I. The values put in square bracket are results obtained in the case that SiO$_2$ layers were also added as fitting parameters.

Layer	Density (g/cm^3)	Thickness (nm)	Roughness (nm)
Tail group	0.93 (0.70)	1.42 (1.64)	0.30 (0.17)
Head group	1.47 (1.58)	0.70 (0.94)	0.30 (0.61)
SiO$_2$	1.77 (2.11)	0.47 (0.35)	0.30 (0.31)
SiO$_2$	2.17 (2.22)	0.53 (0.63)	0.15 (0.00)
Si	2.33	---	0.00

incidence angle lower than $\alpha = 2.5°$ is nearly identical to the fitting curve, while any parameters were unable to reproduce the broad peak at the glancing incidence angle of $\alpha = 2.5 \sim 4.0°$. Although good fitting curves were obtained for the case that a SiO$_2$ layers were also fitted (not shown in this report), they were not acceptable values for the following reasons. For instance, the density parameters were not identical to that experientially known tendency, i.e., the density of SiO$_2$ placed at an inside region was higher than that of the other SiO$_2$ layer placed at an outside region, or SiO$_2$ layers became higher than a Si substrate. The above results mean that model I failed in reproducing the

actual layer structures for both films, with respect to the electron density contrast in vertical direction to a film surface. This result, in turn, demonstrates that specular X-ray reflectivity profiles reflect electron density contrast even in a monolayer film!

In order to evaluate an electron density contrast in the direction of surface normal, model II, in which a monolayer was divided into two layers consisting of tail and head groups, was applied as a structure model using the constant parameters for SiO$_2$ layers. Under these conditions, good fitting results for the SXR profiles of both LB films were obtained as shown in Figs. 5 (a) and (b). We also fitted the profiles by changing the

parameters concerning not only tail and head group layers but also two SiO_2 layers. Identical fitting curves were also obtained (calculated curves were not shown in this report). Results of fitting parameters are arranged in Table III (a) and (b). In the case of $[Ru(bpy)_2(dC18bpy)]^{2+}(ClO_4)_2$ LB film, some of the parameters slightly changed from the case that oxide layers are fixed at constant values, while in the case of $[Ru(phen)_2(dC18bpy)]^{2+}(ClO_4)_2$ LB film, the obtained parameters are almost identical between these two fitting procedures. Taking the experientially known property of naturally produced SiO_2 layer and size of complex molecules into account, acceptable values were obtained in all cases that applied a model II,.

It seems that model II and parameters given by fitting procedure can illustrate their film structure. It should be mentioned that model II is not a unique model because there still remain a lot of models to be examined. It is not realistic, however, to examine all possible structural models. We should note that the calculation was just carried out under the assumption based on molecular model and sample preparation process. Regarding present samples, Langmuir film transfer took place at updrowing process of substrate from subphase, i.e., molecules were expected to contact head group with hydrophilic Si substrate surface. In addition, we have to pay attention that it becomes easier to fit calculation to raw reflectivity curve with increasing the number of parameters as seen in applying a model I. In that case, good fitting curves were obtained by adding SiO_2 layers as fitting parameters. Since anomalous values were found in that result fortunately, we could eliminate that model.

4. CONCLUSION

We tried to apply specular X-ray reflectometry to estimate a molecular orientation in monolayer films, taking an electron density profile into account. As a result, reflectivity profile has been revealed to reflect electron density contrast caused by molecular orientation even in the monolayer film. All we can conclude is that model I which assumes a random orientation model did not reflect the right film structure, since a lot of models to be examined still remain. Through the present report, we would like to mention some problems in regard to interpretation of SXR profiles. Theoretically any structure model could reproduce an observed reflectivity profile when a sufficient number of parameters with any value are used. In some fortunate cases, however, we are able to verify the results with help of knowledge about the actual properties of a given sample. For this reason, we should discuss and make effort to establish a novel optical theory by putting together various optical

theories to express an electron density profile in a monolayer without dependence on structural model or much knowledge of sample.

Finally we wish to point out that although a lot of problems still remain in analysis of specular X-ray reflectivity curves, at least it can complementarily support other spectroscopic techniques for estimation of molecular orientation in a film. It has much possibility in that purpose, since X-ray well reflects electron density profile and distribution.

Reference

[1] R. G. Greenler, *J. Chem. Phys.*, 44, 310-315, (1966).

[2] W. Hansen, *Symp. Faraday, Soc.*, 4, 27-35 (1970).

[3] T. Hasegawa, S. Takeda, A. Kawaguchi, J. Umemura, *Langmuir*, 11, 1236-1243 (1995).

[4] T. Iwashita, X.Xia, *J. Electroanal. Chem.*, 411, 95-102, (1996)

[5] M. Osawa, *Bull. Chem. Soc. Jpn.*, 70, 2861-2880, (1997)

[6] P. Guyot-Sionnest. P. H. Lin, E. M. Hiller, *J. Chem. Phys.*, 102 4269-4278, (1995).

[7] P. Hébert, A. L. Rille, W. Q. Zheng, A. Tadjeddine, *J. Electroanal. Chem.*, 447, 5-9, (1998).

[8] K. Domen, A. Bandara, J. Kubota, K. Onda, A. Wada, S. S. Kano, C. Hirose, *Surf. Sci*, 427-428, 349-357 (1999).

[9] L. G. Parratt, *Phys. Rev.*, 95 359-369, (1954).

[10] L. Nevot, P. Croce, *Rev. Phys. Appl.*, 15, 761-779, (1980).

[11] B. M. Ocko, J. Wang, A. Davenport, H. Isaacs, *Phys. Rev. Lett.*, 65, 1466-1469.

[12] K. Sakurai, A. Iida, *Jpn. J. Appl. Phys.*, 31, L113-L115, (1992).

[13] N. Awaji, Y. Sugita, S. Ohkubo, T. Nakanishi, K. Takasaki, S. Komiya, *Jpn. J. Appl. Phys.*, 34, L1013-L1-1016, (1995)

[14] H. Yamaoka, H. Matsuoka, K. Kago, H. Endo, J. Eckelt, R. Yoshidome, *Chem. Phys Lett.*, 295, 245-248, (1998).

[15] G. Evmenenko, M. E. van der Boom, J. Kmetko, S. W. Dugan, T. J. Marks, P. Dutta, *J. Chem. Phys.*, 115, 6722-6727, (2001).

[16] S. Takahashi, M. Taniguchi, K. Omote, N. Wakabayashi, R. Tanaka, A. Yamagishi, *Chem. Phys. Lett.*, 352, 213-219, (2002).

[17] M. Mizusawa, K. N. Stoev, K. Sakurai, *Jpn. J. Appl. Phys.*, 42, 3709-3710, (2003).